



CONFERENCE PAPER

Characterization and optimization of palm industry ash waste (PIAW) derived zeolites using central composite design (CCD)

Said Nurdin^{1,*}, Syafiqah A. Khairuddin¹, Hajar Athirah M. Sukri¹, Chuah C. Wooi²

¹ Faculty of Chemical & Natural Resources Engineering, Universiti Malaysia Pahang (UMP), Lebuhraya Tun Razak, 26300 Gambang, Kuantan, Pahang, MALAYSIA

² CH Biotech Sdn Bhd, Kancil str. 3&4, 36400 Hutan Melintang, Teluk Intan, Perak, MALAYSIA

ABSTRACT

The prodigious ashes from power electricity generation plants were devastated as solid waste by palm industries into environment. PIAW, mostly Palm Oil Fuel Ash (POFA) comprising silica and alumina was discarded as non-profit oriented products, thus this work is about PIAW, essentially POFA derived zeolites using ultrasound irradiation. Performance of POFA was characterized, and process optimization was done by employing CCD. Pre-treated POFA as feedstock and formed zeolites were designated and analyzed using X-Ray Fluorescence (X-RF), Scanning Electron Microscopy (SEM) images, Fourier Transform Infrared (FTIR) spectrum and X-Ray Diffraction (XRD) diagram. Alkaline concentration (0.6 M-1.4M), irradiation time (140 min-160 min) and KOH/POFA (1.5:1-2.5:1) were examined as non-constant variables. Otherwise, ultrasonic power (600W), temperature (80°C) and silica alumina ratio were justified as constant and response variables. An optimal synthesized zeolites as ratio of SiO₂ and Al₂O₃ (10.60) was found from surface plot based on quadratic typical at KOH=1 M, KOH/POFA=2 and time=150 min. Presence of A, P, X and irregular shape structures zeolites are commensurable to another resources, mainly fly ash. These findings are also important for waste reduction, recycling and zeolites synthesis from material under economic value.

Keywords: Quadratic model, ultrasound irradiation, alkaline, waste recycling, silica

1. INTRODUCTION

Palm industry ash waste (PIAW) is a by-product from palm oil mills, resulted from combustion of palm shell and bunches for steam generation. PIAW which is palm oil fuel ash (POFA) was devastated as solid waste by palm oil industries. There have been certain ways of the PIAW abundant utilization and treatment such as act as fuel sources in oil palm mill and dumped in landfill. Unfortunately, the PIAW usage for electricity generation via combustion process does not enough due to dispose of approximately 0.25 million tons in landfills [1]. Efforts for PIAW utilization via production of value-added materials have been being done i.e. additive in concrete and cement [4], [5], masonry building blocks [6], adsorbent [7] and filler in natural rubber [8] etc. Alternatively, conversion of PIAW to zeolite could be processed, and it enables the industries to develop the

under economic value waste to powerful materials. Previous researchers related with solid waste zeolites from various resources and techniques have been being developed [9], [10].

Zeolites are one of micro-porous materials that commercially used as catalysts and adsorbents like gas separation, etc. Framework of zeolite comprises of three-dimensional connection of SiO₄ and AlO₄ tetrahedra through shared oxygen atoms forming many regular arrangements resulted to an open crystal lattice. As the substitution of an AlO₄ tetrahedron for a SiO₄ tetrahedron, negative charge was created [11]. The crystalline aluminosilicate material has an intense acid strength and a regular molecular sized-pore structure of hydrocarbons [12]. There are several forms of zeolites such as limonite, X-type, Y-type, sodalite and calcium aluminosilicate. Zeolites are commonly synthesized using hydrothermal approach at 200 °C in an alkaline

Corresponding Author: snurdin2@gmail.com (Said Nurdin)

Received 11 July 2018; Received in revised form 21 October 2018; Accepted 21 October 2018

Available Online 31 October 2018

Doi: ISSN: 2636-8498

© Yildiz Technical University, Environmental Engineering Department. All rights reserved.

This paper has been presented at EurAsia Waste Management Symposium 2018, Istanbul, Turkey

medium condition. At similar conditions, different types of zeolites from various sources can be produced. Moreover, the zeolites synthesis were also conducted at temperature range of 90°C-200°C [13], [14]. However, the hydrothermal methods required energy-intensive and time-consuming. Ultrasonic approach could be used to minimize the supplied energy and enforced time [15]. The application of ultrasound for chemical reactions and processes is termed as sonochemistry. Presence of ultrasound during crystallization may affect the physicochemical phenomena which connected to nucleation and crystal growth. The sonification plays crystallization time and temperature reduction many roles, and it can increase the degree of zeolites crystallinity [16]. This paper reported about characterization and optimization of zeolite synthesis from PIAW, mostly POFA using CCD. Effects of KOH/POFA ratio, irradiation time and alkaline-KOH concentration as non-constant variables were investigated.

2. MATERIALS AND METHODS

2.1. Materials

The PIAW, mostly POFA was supplied by CH Biotech Sdn Bhd, Teluk Intan, Perak, Malaysia. Potassium hydroxide was ordered by Permula Sdn Bhd, Kuantan, Malaysia. The commercialized zeolites was provided by Gelanggang Kencana, Sdn Bhd, Malaysia.

2.2. Methods

2.2.1. Pre-treatment and performance of PIAW

The PIAW, principally POFA was dried and sieved for foreign and uncombusted palm fibres separation. Next, the used samples were ground for pozzolanic reaction enhancement. Calcination of PIAW was conducted by using a muffle furnace at 800°C for 2 hours. This treatment was subjected to remove unburnt carbon, volatiles matters and others impurities removal. The POFA performance was then identified using X-Ray Fluorescence (XRF), Fourier Transform Infrared (FTIR) and Scanning Electron Microscopy (SEM) for composition, infrawave and morphological identification.

2.2.2. Experimental procedure

In mixing steps, potassium hydroxide (analytical grade) was agitated with deionized water. Then, the POFA and KOH were mixed in supersonic device with specification of adjustable Crest Ultrasonic P1800D, like power and temperature (Fig 1). The temperature was set up constant by heater and controller. Frequency and ultrasonic wave power of 45 kHz and 600 W were arranged respectively. Irradiation time (140 min-160 min), alkaline concentration (0.6 M-1.4 M) and KOH/POFA ratio (1.5:1-2.5:1) were preferred as altered variables. Ultrasonic power (600 W), operation temperature (80°C) and silica alumina ratio were substantiated as constant and response variables. The mixture was then filtered to obtain solids of synthesized zeolites and washed until

neutral. Obtained filtrate was dried, grinded and stored in desiccator prior to use. The resulted zeolites were then characterized and analyzed.



Fig 1. Crest Ultrasonics P1800D for PIAW derived zeolites optimization

2.2.3. Zeolites characterization

Zeolites characterization was carried out based on obtained optimal process parameters. Morphology, infrared spectra, and X-ray diffraction of synthesized zeolites were recognized and compared with others. Zeolites types, texture and phases were also discovered. Silica and alumina ratio was subjected to ascertain the resulted zeolites interpretation.

2.2.4. CCD optimization

CCD via Design Expert 7 program comprising 15 runs was employed for analysis of optimal synthesized zeolites. The lay out from CCD was tabulated by test run, KOH/PIAW ratio, ultrasonic exposure time and KOH concentration. Five levels with five replicates at the central point, and these set points for each variables with low (coded value: -2) and high value (coded value: +2) were applied, as shown in Table 1.

Response of the experiments was analyzed based on $\text{SiO}_2/\text{Al}_2\text{O}_3$. The highest silica per alumina ratio was selected as the best condition from PIAW conversion to zeolites. Validated three times of experimental results were approved for process parameter optimization. In front of the terms, positive sign attributed to synergistic effects on the silica-alumina ratio as synthesized zeolites.

Error analysis was calculated between predicted and experimental values as given in the following equation 1.

$$\text{Experimental error (\%)} = \frac{\text{Experimental} - \text{Predicted}}{\text{Experimental}} \times 100\% \quad (1)$$

Effect of the chosen variables and the interaction with each other by obtained silica-alumina ratio as zeolites was illustrated in three-dimensional surface diagram. The results of the CCD were identified and interpreted

by analysis of variance (ANOVA), and coefficient R^2 and R^2 adjusted determination were run by Design Expert 7. Empirical equation was determined by the Fisher variance ratio (the F-test value) for

examination of created model. The CCD has also been being widely applied in various adsorption, separation, etc. for optimization [17], [18].

Table 1. The manipulated optimization variables using CCD

Optimized variables	Coded factor levels				
	-2	-1	0	+1	+2
A: KOH/POFA	1.5:1	1.75:1	2:1	2.25:1	2.5:1
B: Irradiation time, min	140	145	150	155	160
C: KOH concentration (M)	0.6	0.8	1	1.2	1.4

3. RESULTS AND DISCUSSION

3.1. Materialization of PIAW

Materialization of PIAW, mainly POFA for zeolites was related on performance analysis. Morphological structure of POFA was distinguished using scanning electron microscopy (Fig 2). The scanning electron diagnosis of POFA shows less fibrous form than cubic structure. Poros characteristics and cubic structure of the PIAW have been found by the SEM image of $\times 1000$. Textures images of POFA revealed diffused melt phase. The POFA has also covered an aluminosilicate glass phase. Absorption band characteristics of POFA were presented by FTIR analysis in Fig 4. Silanol group, Si-OH was reflected by stretch band at 3447.80 cm^{-1} . This band was reported which present in range of $3200\text{-}3750 \text{ cm}^{-1}$. The unique characteristics were also found around $1300\text{-}1400 \text{ cm}^{-1}$ that belongs to alcohol and phenol on adsorbent surface. Al_2O_3 also included in this adsorption band at $550\text{-}875 \text{ cm}^{-1}$. XRD diagram of POFA was illustrated in Fig 5, which it predominantly consisted of aluminosilicate-glass, quartz and mullilite. These structures were almost similar with fly ash. Broad hump around $20^\circ\text{-}22^\circ$ and $15^\circ\text{-}40^\circ$ stipulated the amorphous identity of POFA [19]. X-RF analysis of POFA could be exhibited with chemical compounds. The chemical contents of POFA were SiO_2 (50.29%), CaO (18,16%), K_2O (7.10%), Al_2O_3 (6.53%), MgO (6.48%), P_2O_5 (5.62%), Fe_2O_3 (4.02%), TiO_2 (0.37%), Na_2O (0.29%), MnO (0.13%) and ignition loss (1.01%). The POFA constituents of SiO_2 , CaO, Al_2O_3 etc. have also been reported by another researchers [20], but the dissimilar composition and characteristics were caused by various operation methods, feedstocks and palm oil plantation areas.

3.2. Zeolites improvization

Zeolites improvization was also conducted by elemental, X-ray diffraction, morphology and infrared. The infrared analysis results of zeolites were displayed in Fig 4. Characteristic bands were commonly stated to spectra of zeolites. The peaks region $650\text{-}720 \text{ cm}^{-1}$ attributed to internal tetrahedral: symmetric stretch, $750\text{-}820 \text{ cm}^{-1}$ corresponded to external tetrahedra: symmetric stretch, and $950\text{-}1250 \text{ cm}^{-1}$ related to internal tetrahedral: asymmetric stretch [21].

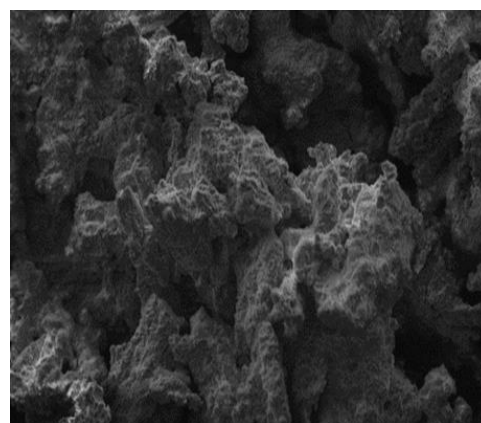


Fig 2. SEM images of POFA at 1000 x magnification

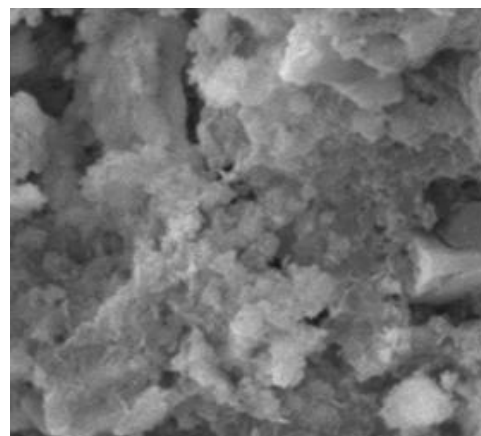


Fig 3. SEM images of zeolites at 1000 x magnification

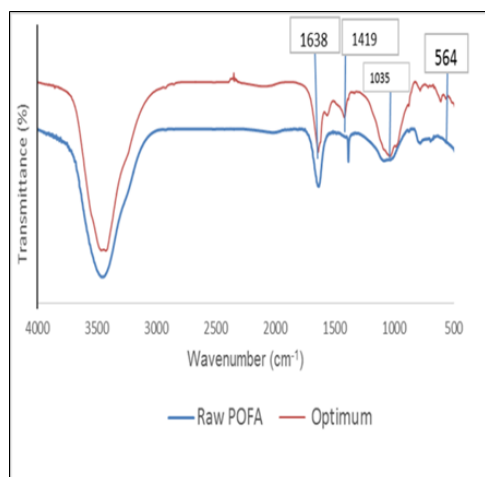


Fig 4. FTIR spectrum of POFA and zeolites (optimum)

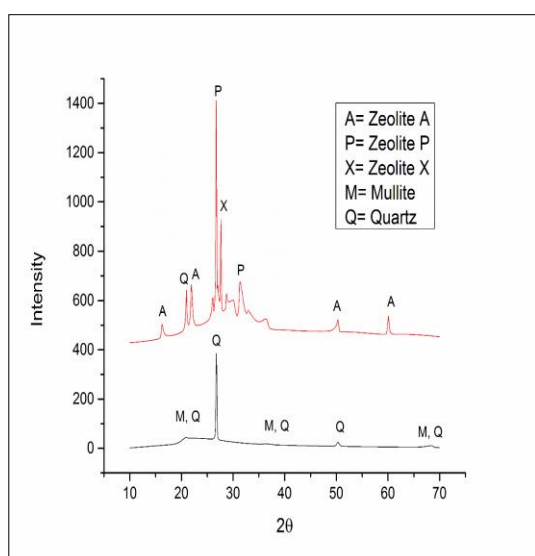


Fig 5. XRD diagram of POFA and zeolites (optimum)

For justification of zeolites presence, there was characteristic peaks within region 420-1200 cm^{-1} , it was IR character of zeolites A [22]. Presence of zeolites A was also supported by characteristic band at 1035 cm^{-1} [23]. Peak at 564 cm^{-1} indicated zeolite X as reported by previous reports [24]. Bands closed to 1419 cm^{-1} , it designated carbonate stretching vibration that facilitated nucleation and zeolites crystallization [25]. The peak at 1638 cm^{-1} was associated with zeolites P [26]. Elemental analysis of zeolites was also governed by SiO_2 , CaO , Al_2O_3 , etc. The $\text{SiO}_2/\text{Al}_2\text{O}_3$ ratio > 5 , it reflected the PIAW, typically POFA conversion with high silica zeolites. Morphology of zeolites was identified by scanning electron microscope with 1000 x magnitudes (Fig 3). The image almost match zeolites A and P as obtained by precursory discoveries [27], [28]. Surface morphology and structural were irregular, rough and different compared raw material. Estimated, it was caused by alkali activation and cavitation bubbles from ultrasonic irradiation. Next, zeolites recognition was also examined using X-ray diffraction (Fig 5). The image indicated presence of zeolite A, P and X. Amorphous phase and high intensity peak obtained were virtually similar to former data [29].

3.3. CCD optimization model

3.3.1. Factorial design and quadratic model

Three factorial design: KOH/POFA ratio (A), ultrasonic time (B) and KOH concentration (C) have been optimized by Response Surface Model (RSM) using CCD. The list of experiments designed by CCD is shown in Table 2. Regression analysis was performed to fit the response variable. The results of the CCD were identified and interpreted by analysis of variance (ANOVA), and the final empirical model is presented as:

$$Y = 10.44 + 0.29A - 0.12B - 0.13C - 0.045AB + 0.045AC + 0.13BC - 0.24A^2 - 0.19B^2 - 0.17C^2 \quad (2)$$

where Y is predicted silica per alumina ratio, A is KOH/POFA ratio, B is irradiation time and C is KOH concentration. In front of the terms, positive sign attributed to synergistic effects on the silica per alumina ratio of the synthesized zeolites. The importance of the empirical model was determined by the Fisher variance ratio (the F-test value). Statistically evaluation was subjected to approve the eligibility of used empirical model based on data variations. The model adequacy was elucidated with ANOVA as presented in Table 3.

Regression parameters of the predicted response surface quadratic model were exhibited. Higher F-value is unity, the more certain of the empirical model is described sufficiently, the data variation and the predicted significant terms of the synthesized zeolites are real. With 95% confidence level, the tested model was significant, and the reflected model F-value was 25.28. Obtained R-square was 0.9785, and the found value of 97.9% from total variation in the silica per alumina responses.

Table 2. Experimental layout from CCD

Test Run	KOH/POFA Ratio	Ultrasonic irradiation time (min)	KOH Concentration (M)
1	2.25	155.00	0.80
2	2.25	145.00	1.20
3	1.75	155.00	1.20
4	1.75	145.00	0.80
5	1.50	150.00	1.00
6	2.50	150.00	1.00
7	2.00	140.00	1.00
8	2.00	160.00	1.00
9	2.00	150.00	0.60
10	2.00	150.00	1.40
11	2.00	150.00	1.00
12	2.00	150.00	1.00
13	2.00	150.00	1.00
14	2.00	150.00	1.00
15	2.00	150.00	1.00

The error analysis of actual compared prediction model was < 10%. There are only a 0.12 % chance that a "Model F-value" was large, it could be occurred due to noise. The obtained value enables the reliable model in estimating the silica per alumina ratio. Significance model was stated with Probability (Prob)>F less than 0.05. Analysis of variance has also been examined for rapid synthesis of zeolites NaA using microwave with a low probability value ($P>F<0$) and the model value $F = 27.88$ exceeded the table value $F=2.72$ [30]. Both results fitted well and specified the model terms were impressive.

3.3.2. Effects of model components

Effects of the chosen variables interactions with silica per alumina ratio as synthesized zeolites were illustrated in three-dimensional surface plot diagram (Fig 6). At ultrasonic exposure time (145-150 min) and KOH/POFA ratio (2.0 - 2.25), it might be achieved the maximum silica per alumina ratio. The silica per

alumina ratio increased up to 10.60, with enlarged KOH/POFA ratio and exposure time. In addition, when KOH concentration, KOH/POFA ratio and irradiation time were extended up to peak, the obtained silica alumina ratio verified optimum value. A good interactions of the two variables within the three-dimensional surface diagram was also assigned by the elliptical shape [31].

3.3.3. Model verification

The CCD model generated during RSM was verified by experiments run for an obsessed optimal medium setting. A KOH concentration of 1 M was found SiO_2 and Al_2O_3 ratio of 10.60 as measured zeolites parameters, at KOH/POFA ratio of 2:1 and irradiation time of 150 min. The experiment was carried out depended on these relevant modes to justify the actual value. The validation data were arrayed in Table 4. Laboratory results revealed SiO_2 and Al_2O_3 of 10.32, which are almost and fitted well with the optimized value using CCD generated by the RSM tool.

Table 3. ANOVA and adequacy of the quadratic model

Source	Sum of squares	Degree of freedom	Mean square	F value	p-value Prob > F
Model	3.08	9	0.34	25.28	0.0012
A	0.68	1	0.68	50.49	0.0009
B	0.11	1	0.11	8.15	0.0356
C	0.14	1	0.14	10.36	0.0235
AB	5.4 E-003	1	5.4 E-003	0.40	0.5557
AC	5.4 E-003	1	5.4 E-003	0.40	0.5557
BC	0.045	1	0.045	3.32	0.1279
A ²	1.31	1	1.31	96.55	0.0002
B ²	0.88	1	0.88	64.98	0.0005
C ²	0.69	1	0.69	50.79	0.0008
Residual	0.068	5	0.014		
Lack of fit	0.014	1	0.014		
Pure error	0.054	4	0.014	1.01	0.3719
Cor total	3.15	14			

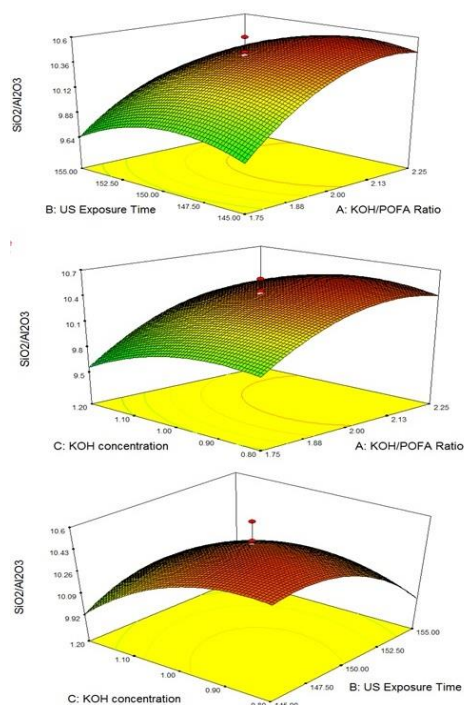


Fig 6. CCD generated response surface plot for PIAW derived zeolites as $\text{SiO}_2/\text{Al}_2\text{O}_3$

Table 4. Optimization results of PIAW derived zeolites as $\text{SiO}_2/\text{Al}_2\text{O}_3$

Optimum validation	Experimental/ Actual	Predicted by RSM Using CCD	% Error
1	10.32	10.60	2.64
2	10.03	10.60	5.38
3	10.14	10.60	4.34

4. CONCLUSIONS

Characterization and optimization of PIAW derived zeolites have been exhibited to be efficacious within 150 min of irradiation time at 80°C. The formed zeolites were found at KOH/POFA ratio (1.5:1 – 2.5:1) and alkaline concentration (0.6 M-1.4 M) at ultrasonic power of 600 W. Zeolites performance and treated PIAW were assessed, which showed that the different morphology, chemical substituent, diffraction, infrared and phases are strictly controlled by synthesis operation parameters. Appearance of A, P and X zeolites and asymmetrical structures are comparable with diversified zeolites waste sources. Effects of used variables and its interactions were tested by analysis of variance. Statistically examinations were significant ($p < 0.05$), and some correlations among each other were disclosed. Experimental results ($\text{SiO}_2 / \text{Al}_2\text{O}_3 = 10.32$) acquired were well matched with the optimized value given by the CCD ($\text{SiO}_2 / \text{Al}_2\text{O}_3 = 10.60$). The resulted zeolites as $\text{SiO}_2 / \text{Al}_2\text{O}_3$ from PIAW substantially POFA could be also optimized using additional statistical methods, like Taguchi, etc.

ACKNOWLEDGMENT

The authors are grateful for sponsorship by the Ministry of Higher Education, Malaysia under Grants FRGS-RDU 160126 & RDU 141005, PRGS 160321&160354, CH Biotech Sdn Bhd for materials providing, Research & Innovation Dept. and Faculty of Chemical & Natural Resources Engineering Laboratory Staff-UMP for technical supports.

REFERENCES

- [1]. A. Kongnoo, S. Tontisirin, P. Worathanakul and C. Phalakornkule, "Surface characteristics and CO2 adsorption capacities of acid- activated zeolite 13X prepared from palm oil mill fly ash," *Fuel*, Vol.193, 385–394, 2017.
- [2]. Z. Y. Lai and S. M. Goh, "Mechanical strength of binary oil palm kernel shell and HZSM-5 zeolite fuel pellets," *Fuel*, Vol.150, 378–385, 2015.
- [3]. N. H. A. S. Lim, M. A. Ismail, H. S. Lee, M. W. Hussin, A. R. M. Sam and M. Samadi, "The effects of high volume nano palm oil fuel ash on microstructure properties and hydration temperature of mortar," *Construction and Building Materials*, Vol.93, 29–34, 2015.
- [4]. M. M. U. Islam, K. H. Mo, U. J. Alengaram and M. Z. Jumaat, "Mechanical and fresh properties of sustainable oil palm shell lightweight concrete incorporating palm oil fuel ash," *Journal of Cleaner Production*, Vol.115, 307–314, 2015.
- [5]. M. Safiuddin, M. Abdus Salam and M. Z. Jumaat, "Utilization of Palm Oil Fuel Ash in Concrete: A Review," *Journal of Civil Engineering and Management*, Vol.17(2), 234–247, 2011.
- [6]. M. E. Rahman, A. L. Boon, A. S. Muntohar, M. N. H. Tanim and V. Pakrashi, "Performance of masonry blocks incorporating Palm Oil Fuel Ash," *Journal of Cleaner Production*, Vol.78, 195–201, 2014.
- [7]. C. Acquah, L. S. Yon, Z. Tuah, N. L. Ngee and M. K. Danquah, "Synthesis and performance analysis of oil palm ash (OPA) based adsorbent as a palm oil bleaching material," *Journal of Cleaner Production*, Vol.139, 1098–1104, 2016.
- [8]. Z. X. Ooi, H. Ismail and A. Abu Bakar, "Characterization of oil palm ash (OPA) and thermal properties of OPA-filled natural rubber compounds," *Journal of Elastomers and Plastics*, Vol.47(1), 13–27, 2015.
- [9]. A. Á. B. Maia, R. F. Neves, Rô. S. Angélica and H. Pöllmann, "Synthesis, optimisation and characterisation of the zeolite NaA using kaolin waste from the Amazon Region: Production of zeolites KA, MgA and CaA," *Applied Clay Science*, Vol.108, 55–60, 2015.
- [10]. L. Deng, Q. Xu and H. Wu, "Science Direct Synthesis of zeolite-like material by hydrothermal and fusion methods using municipal solid waste fly ash," *Procedia Environmental Sciences*, Vol.31, 662–667, 2016.
- [11]. N. Al-Jammal, Z. Al-Hamamre and M. Alnaief, "Manufacturing of zeolites based catalyst from

- zeolites tuft for biodiesel production from waste sunflower oil," *Renewable Energy*, Vol.93, 449–459, 2016.
- [12]. G. Watanabe, Y. Nakasaka, T. Taniguchi, T. Yoshikawa, T. Tago and T. Masuda, "Kinetic studies on high-pressure methylation of 2-methylnaphthalene over MTW-type zeolites with different crystal sizes," *Chemical Engineering Journal*, Vol.312, 288–295, 2017.
- [13]. J. C. Kim, M. Choi, H. J. Song, J. E. Park, J. H. Yoon, K. S. Park and D. W. Kim, "Synthesis of uniform-sized zeolite from windshield waste," *Materials Chemistry and Physics*, Vol.166, 20–25, 2015.
- [14]. P. Roy and N. Das, "Ultrasonic assisted synthesis of Bikitaite zeolites: A potential material for hydrogen storage application," *Ultrasonics Sonochemistry*, Vol.36, 466–473, 2017.
- [15]. J. Behin, H. Kazemian and S. Rohani, "Sonochemical synthesis of zeolite NaP from clinoptilolite," *Ultrasonics Sonochemistry*, Vol.28, 400–408, 2015.
- [16]. N. E. Gordina, V. Y. Prokof'Ev, Y. N. Kul'Pina, N. V. Petuhova, S. I. Gazahova and O. E. Hmylova, "Effect of ultrasound on the synthesis of low-modulus zeolites from a metakaolin," *Ultrasonics Sonochemistry*, Vol.33, 210–219, 2016.
- [17]. B. Sadukhan, N. K. Montal and S. Chatteraj, "Optimization using central composite design and desirably function for sorption of methylene blue from aqueous solution onto *Lemna major*," *Karbala International Journal of Modern Science*, Vol.2(3), 145–155, 2016.
- [18]. N. F. Ramandi, A. Ghassempous, N. M. Najafi and E. Gashemi, "Optimization of ultrasonic assisted extraction of fatty acids from *Borago officinalis* L. flower by central composite design," *Arabian Journal of Chemistry*, Vol.10(1), S23–S57, 2017.
- [19]. M. A. Salih, A. A. A. Ali and N. Farzadnia, "Characterization of mechanical and microstructural properties of palm oil fuel ash geopolymer cement paste," *Construction and Building Materials*, Vol.65, 592–603, 2014.
- [20]. A. S. A. Aziz, L. A. Manaf, H. C. Man and N. S. Kumar, "Kinetic modeling and isotherm studies for copper (ii) adsorption onto Palm Oil Boiler Mill Fly Ash (POFA) as a natural low-cost adsorbents," *Bioresources*, Vol.9(1), 336–356, 2014.
- [21]. N. M. Musyoka, L. F. Petrik, E. Hums, H. Baser and W. Schwieger, "In situ ultrasonic diagnostic of zeolite X crystallization with novel (hierarchical)," *Ultrasonics*, Vol.54(2), 537–543, 2014.
- [22]. M. P. Moisés, C. T. P., Da Silva, J. G. Meneguim, E. M. Girotto and E. Radovanovic, "Synthesis of zeolite NaA from sugarcane bagasse ash," *Materials Letters*, Vol.108, 243–246, 2013.
- [23]. M. Gougazeh and J. C. Buhl, "Synthesis and characterization of zeolite A by hydrothermal transformation of natural Jordanian kaolin," *Journal of the Association of Arab Universities for Basic and Applied Sciences*, Vol.15(1), 35–42, 2014.
- [24]. C. Santasnachok, W. Kurniawan and H. Hinode, "The use of synthesized zeolites from power plant rice husk ash obtained from Thailand as adsorbent for cadmium contamination removal from zinc mining," *Journal of Environmental Chemical Engineering*, Vol.3(3), 2115–2126, 2015.
- [25]. S. S. Bukhari, J. Behin, H. Kazemian and S. Rohani, "Conversion of coal fly ash to zeolite utilizing microwave and ultrasound energies: A review," *Fuel*, Vol.140, 250–266, 2015.
- [26]. S. N. Azizi and N. Asemi, "The effect of ultrasonic and microwave-assisted aging on the synthesis of zeolite P from Iranian perlite using box-behken experimental design," *Chemical Engineering Communications*, Vol.201(7), 909–925, 2014.
- [27]. S. Bohra, D. Kundu and M. K. Naskar, "One-pot synthesis of NaA and NaP zeolite powders using agro-waste material and other low cost organic-free precursors," *Ceramics International*, Vol.40(1), 1229–1234, 2014.
- [28]. T. V. Ojumu, P. W. Du Plessis and L. F. Petrik, "Synthesis of zeolite A from coal fly ash using ultrasonic treatment - A replacement for fusion step," *Ultrasonics Sonochemistry*, Vol.31, 342–349, 2016.
- [29]. T. Aldahri, J. Behin, H. Kazemian and S. Rohani, "Synthesis of zeolite Na-P from coal fly ash by thermo-sonochemical treatment," *Fuel*, Vol.182, 494–501, 2016.
- [30]. N. Sapawe, A. A. Jalil, S. Triwahyono, M. I. A. Shah, R. Jusoh, N. F. M. Salleh, B. H. Hameed and A. H. Karim, "Cost-effective microwave rapid synthesis of zeolite NaA for removal of methylene blue," *Chemical Engineering Journal*, Vol.229, 388–398, 2013.
- [31]. E. A. Mohamed, A. Q. Selim, M. K. Seliem and M. R. Abukhadra, "Modeling and optimizations of phosphate removal from aqueous solutions using synthetic zeolite NaA," *Journal of Materials Science and Chemical Engineering*, Vol.3, 15–29, 2015.